Desalination and Water Treatment
www.deswater.com

doi:10.5004/dwt.2018.22706

120 (2018) 9–15
July

Effect of microbubbles on membrane fouling due to protein in water treatment processes

Tomoichi Watabe[a], Tomoki Takahashi[a,b], Kazufumi Matsuyama[a], Hideto Matsuyama[a,*]

[a]*Center for Membrane and Film Technology, Department of Chemical Science and Engineering, Kobe University, 1-1 Rokkodaicho, Nada-ku, Kobe 657-8501, Japan, Tel. +81-78-803-6180, Fax +81-78-803-6180, email: tm_watabe@daicen.daicel.com (T. Watabe), Tel. +81-47-474-2859, Fax +81-47-473-1227, email: takahashi.tomoki@nihon-u.ac.jp (T. Takahashi), Tel. +81-78-803-6180, Fax +81-78-803-6180, email: budouhitotsubudou@gmail.com (K. Matsuyama), Tel. +81-78-803-6180, Fax +81-78-803-6180, email: matuyama@kobe-u.ac.jp (H. Matsuyama)*
[b]*College of Industrial Technology, Nihon University, 2-11-1 Shin-ei, Narashino, Chiba275-8576, Japan*

Received 25 March 2018; Accepted 25 June 2018

ABSTRACT

In water treatment processes, an ultrafiltration (UF) membrane is usually used for drinking water production from surface water and for reclaimed water production from wastewater. Membrane fouling due to the deposition of various foulants on the UF membrane surface and pore blocking is a major problem. It has already reported that application of microbubbles (MBs) reduces the fouling. However, the mechanism is not clear yet. Thus, in this study, the mechanism of reducing fouling, especially the fouling due to proteins, by MBs was investigated using bovine serum albumin (BSA) as a model foulant. The filtration was done with a cross flow filtration unit. MBs were applied into the feed solution just before the inlet of UF module. A retentate and an overflow were returned into the feed tank. It was found that BSA were denatured and coagulated by the application of MBs. The coagulated BSA floated in the feed tank and then, the BSA concentration at the bottom of feed tank decreased. Thus, when the feed was suctioned from the bottom of feed tank, the fouling was reduced as well as a decrease in BSA concentration.

Keywords: Microbubbles; Membrane fouling; BSA; Floatation; Aggregation

1. Introduction

In recent years, membrane processes have attracted worldwide attention in both scientific and industrial fields, and have been used in numerous applications such as water treatment including drinking water and wastewater, food industry and so on. In water treatment processes, an ultrafiltration (UF) membrane is usually used for drinking water production from surface water and for reclaimed water production from wastewater. In water treatment processes with UF membrane, however, a membrane fouling due to deposition of various foulants on membrane surface and pore blocking is a major problem. The membrane fouling deteriorates product quality, reduces permeation flux, and thus increases energy consumption. In addition, it results in frequent chemical cleaning of membranes and membrane module replacement. Thus, the fouling results in an increase of water production costs. Therefore, it is essential to prevent the fouling for reducing water production costs.

Natural organic matters (NOMs) such as humic substances, proteins, and polysaccharides are widely recognized as major foulants in low-pressure membrane processes such as UF in surface water treatment [1,2]. Hydrophobichumic substances have been considered as dominant foulants in UF membrane process [3]. On the other hand, it is also reported that polysaccharides and proteins are problematic foulants in UF process in spite of their relatively hydrophilic characters [1,2]. In addition, biopolymers detected by the liquid chromatogra-

*Corresponding author.

phy-organic carbon detection (LC-OCD) which consist of polysaccharides and proteins are also considered as main foulants [4]. These foulants in the surface water come from not only natural matters but also industrial wastewaters effused to rivers. Especially, the wastewater in milk industries contains a lot of protein. Inadequately treated wastewater causes bad odor and badly affects a substrate of fish. Thus, this inadequately treated wastewater is considered as one of the factors causing deterioration of environment [5].

The membrane fouling is generally classified into a reversible fouling and an irreversible fouling. The reversible fouling is possible to recover by a physical treatment such as a back washing of membrane. However, the irreversible fouling cannot be recovered by the physical treatment. Thus, the irreversible fouling is the most severe problem [6,7]. One of the possible ways to reduce the irreversible fouling is the reduction of NOM content of raw water. A pretreatment of raw water has a high potentiality for reducing NOM content. Coagulation/sedimentation through addition of chemicals is the most common pretreatment not only for improving the quality of treated water but also for reducing the membrane fouling [8,9]. However, coagulation/sedimentation has various problems, such as a high flocculant cost and a subsequent membrane fouling by residual flocculants [10,11].

Recently, some chemical-free processes have been reported for membrane fouling reduction. Hallé et al. reported the chemical-free rapid biological filtration for surface water treatment [12]. Although the contact time with the biofilter was long, the membrane fouling was reduced. Muthukumaran et al. used an ultrasonic cleaning to reduce the membrane fouling in whey treatment [13]. We have also reported that microbubbles (MBs) are effective for reducing membrane fouling in the UF process of surface water, for example, the membrane fouling due to biopolymers in river water [14]. In a pilot-scale membrane filtration of river water using a module with an effective membrane area of 5.0 m^2, the stable membrane filtration was achieved under a high membrane flux of 3.0 $m^3/(m^2\ day)$ by adding MBs to feed water [15]. Thus, MBs are also effective for a chemical-free fouling reduction. However, the mechanism of fouling reduction by MBs is not clear yet. In this study, we investigate the mechanism of fouling reduction by MBs, especially fouling due to protein, using a bovine serum albumin (BSA) as a model foulant.

2. Experimental

2.1. Materials

Model feed solution in filtration experiments were prepared by dissolving BSA (Wako Pure Chemical Industries, Osaka, Japan) in deionized water. Suwannee River Humic Acid Standard II (SR-HA) (International Humic Substances Society, Colorado, USA), Guar Gum (Ina Food Industry Co., Nagano, Japan) and BSA were used in the Quartz Crystal Microbalance with Dissipation monitoring system (QCM-D) measurement. SR-HA, Guar Gum, and BSA were selected as model foulants because they have been adopted in many studies as examples of humic substances, polysaccharides, and proteins, respectively [16,17].

2.2. Filtration experiments

Fig. 1 shows the schematic diagram of laboratory-scale filtration equipment with the MBs generator. The average MB size was 0.6 mm, and Fig. 2 shows the bubble size distribution. The filtration system was an internal pressure type cross flow unit. The circulation loop comprised a membrane module, an MBs generator, and a feed tank.

The membrane was a cellulose acetate ultrafiltration hollow fiber membrane (Daicen Membrane-Systems Ltd., Tokyo, Japan) with 0.80/1.30 mm in inner/outer fiber diameters and 110 mm in length. One hollow fiber was set in a pencil-type housing. Then, its effective membrane area was 0.00028 m^2. The nominal molecular weight cut-off (as determined by protein rejection) was 150,000 Da. The membrane

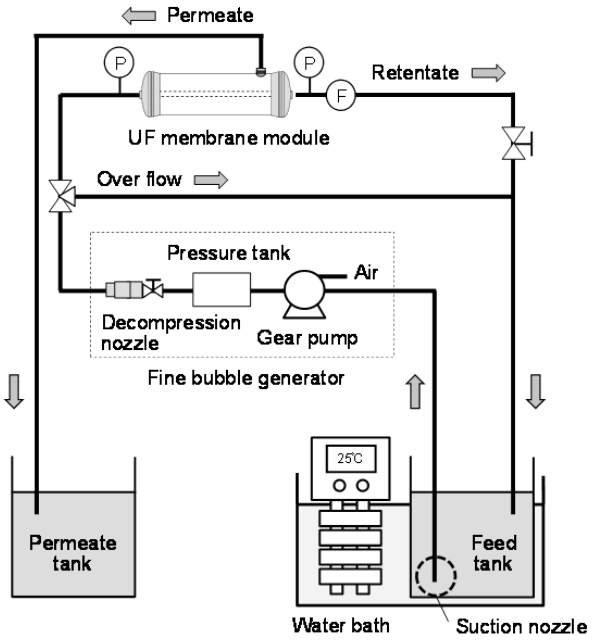

Fig. 1. Schematic diagram of laboratory-scale filtration equipment with the microbubble generator.

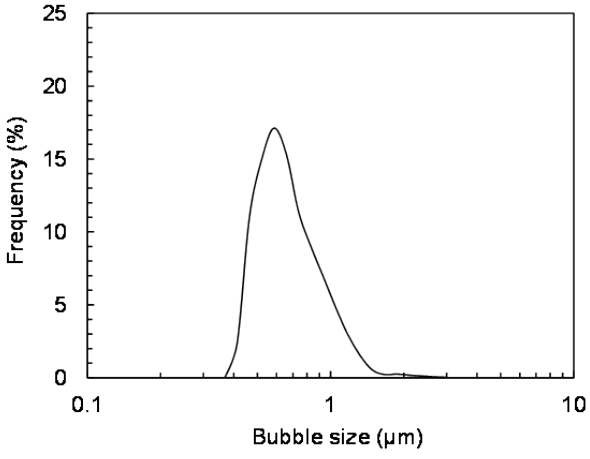

Fig. 2. Distribution of MB size in pure water.

was hydrophilic and had a high antifouling property. The hydraulic permeability of the membrane determined with pure water was 320 L/(m²·h) at 0.5 bar.

The MBs generator was a pressurized dissolution-type apparatus (OM4-MDG-045, AuraTec Co., Ltd., Fukuoka, Japan). Water and air was mixed by the gear pump and supplied to the pressure tank of MBs generator as shown in Fig. 1. The mixture of water and air was pressurized in the pressure tank, where dissolved air was supersaturated. Highly pressurized water was released into the supply pipe through the decompression nozzle and then MBs were generated by discharging the pressure.

At first, pure water was used as feed water and put into a feed tank kept at 25°C. Then, the cross-flow filtration was carried out under a constant pressure of 0.5 bar (flow velocity was almost 0.06 m/s). The retentate and the over flow were circulated to the feed tank and agitated the feed solution. The volume of feed solution was 2 L. Thus, the feed solution stayed in the feed tank for about 1 min. During the filtration, MBs were continuously supplied to the water sample. The volumetric flow rate (mL/min) was determined by measuring the volume of permeate with time. It was confirmed that the MBs did not influence the filtration flux at all in the filtration of pure water containing them. Then, the feed was changed to the sample water and the volumetric flow rate was measured.

In this study, the effect of MBs on reducing membrane fouling was investigated with the total fouling index (TFI) using BSA as a model foulant. TFI is generally used to evaluate the fouling property of a membrane [18–21]. TFI is the sum of hydraulic reversible fouling index (HRFI) and hydraulic irreversible fouling index (HIFI), and is defined as follows [14]:

The specific flux J_s (L/(m² h bar) is given by Eq. (1).

$$J_s = \frac{J}{\Delta P} = \frac{1}{\mu\left(K_{mem} + k_{total}V(t)\right)} \tag{1}$$

where J indicates the water flux (L/(m² h)), ΔP the transmembrane pressure (bar), μ the viscosity of water (bar·h), K_{mem} is the resistance of a clean membrane (m²/L), k_{total} is the sum of rate constants for resistances (m⁴/L²) due to reversible fouling and irreversible fouling, and $V(t)$ is the total permeate volume per unit membrane area (L/m²) during time, t [18–21]. The normalized specific flux (J_s') was obtained by dividing J_s at time, t, $(J/\Delta P)_t$ by J_s at $t = 0$, $(J/\Delta P)_0$ where $V(0)$ is zero as follows:

$$J_s' = \frac{\left(J/\Delta P\right)_t}{\left(J/\Delta P\right)_0} = \frac{1}{1 + \frac{k_{total}}{K_{mem}}V(t)} \tag{2}$$

$$\frac{1}{J_s'} = 1 + \frac{k_{total}}{K_{mem}}V(t) \tag{3}$$

In Eqs. (2) and (3), k_{total}/K_{mem} is the gradient of $1/J_s'$ vs $V(t)$ curve and stands for the total fouling index (TFI).

Table 1 shows the experimental conditions.

2.3. Adsorption of BSA on air/solution interface and onto membrane surface

In order to evaluate the effect of MBs on membrane fouling due to BSA, it is important to understand the adsorption of BSA on air/solution interface corresponding to MBs surface and onto membrane surface. The adsorption of BSA on air/solution interface was evaluated by the surface tension of BSA solution. The surface tension was measured by the pendant drop method with a contact angle meter (DM-300, Kyowa Interface Science, Saitama, Japan) [22,23]. 1000 ppm BSA solution was put into 1 mL syringe and 16 μL droplet was formed using syringe needle, 18G (inner diameter: 0.86 mm, outer diameter: 1.46 mm). The droplet was left to stand and the dynamic surface tension was measured for 1 h. The surface tension, γ (mN/m) was obtained with Eq. (4).

$$\gamma = g\rho de^2/H \tag{4}$$

Here, g indicates the gravitational acceleration (m/s²), ρ the density of droplet (= 1000 kg/m³), de the maximum diameter (m) of droplet and H the correction term obtained from ds/de where ds indicates the diameter of droplet at the position of de from the bottom of droplet. We used the correction term reported in the literature [23].

The adsorption of foulant on the membrane surface was measured by QCM-D method. 1.0 wt% cellulose acetate (CA)/1-methyl-2-pyrrolidinone (NMP) solution was prepared by dissolving powder CA, LT-105 (Daicel Corporation, Osaka, Japan) into NMP. A quartz crystal unit sensor (QSX301, Q-sense) was coated with 1.0 wt% CA/NMP solution by spin coating at 6000 rpm for 60 s, since we used the cellulose acetate UF membrane. The coated sensor was dried at 120°C for 30 min on a hot plate and then used as a CA sensor.

Table 1
Experimental conditions

Case	BSA concentration	Feed solution pretreatment	Section nozzle position	Filtration operation	
				MB supply	System
1	10 ppm	No	Bottom of feed tank	No	Circulate
2	10 ppm	No	Bottom of feed tank	Yes	Open
3	10 ppm	No	Bottom of feed tank	Yes	Circulate
4	10 ppm	MB supply at 30 min	Bottom of feed tank	No	Circulate
5	10 ppm	No	Bottom of feed tank	No	Circulate
6	10 ppm	MB supply at 30 min	Upper part of feed tank	No	Circulate

The QCM-D measurement was done with Q-Sense Explorer model E1 (MEIWAFOSIS CO., LTD., Tokyo, Japan). At first, Milli-Q water was supplied to the module at 50 µL/min for several hours to stabilize the system, after which the CA sensor was set in the chamber. Then, the change of frequency, Df (Hz) was measured for 3 h supplying a foulant solution into the module. 1000 ppm aqueous solutions of BSA, Guar Gum and SR-HA were used as model foulants. The adsorbed amount of foulant (Dm) on the CA sensor was obtained from Df using Sauerbrey's equation:

$$Dm = Dm_t - Dm_0 = -C\,(Df_t - Df_0)/n \quad (5)$$

where C indicates the intrinsic constant of gold sensor (17.7 ng/(cm^2 Hz)) with fundamental frequency of 4.95 MHz and n the overtone (1, 3, 5, 9,11, 13, 15). Dm_0 indicates the coating amount of CA on gold sensor and Dm_t indicates the total amount of absorbed matter on gold sensor.

Df_t and Df_0 are the frequencies at time t and time zero.

2.4. Concentration and conformation of BSA in the feed

The concentration and the conformation of BSA in the feed were investigated, since MBs may affect the denaturation and the coagulation of BSA. The sample was always extracted from the bottom part of feed tank and analyzed without pre-filtration. The concentration of BSA was evaluated from the total organic carbon (TOC). The TOC in feed water was obtained by deducting an inorganic carbon (IC) from a total carbon (TC). IC was analyzed by CO_2 gas generated under pH less than 3. TC was analyzed by CO_2 gas generated by burning at 680°C. IC and TC were measured using TOC-VCSH (SHIMADZU Corporation, Kyoto, Japan).

The size distributions of aggregated BSA was measured using NanoSight NS500 (Quantum Design Japan, Inc., Tokyo, Japan) nanoparticle size analyzers. The tracking number of particles was set over 1000.

The conformation change of secondary structure of BSA was measured with Circular Dichroism (CD) spectrometer, J-725K (JASCO Corporation, Tokyo, Japan). It is possible to predict the protein secondary structure from CD spectrum, since there is a difference in absorbance between right and left circular polarizations depending on the secondary structure of peptide chains [24,25]. The measurement was done using the cell of 1 cm optical length at 25°C.

3. Results and discussion

3.1. Effect of MBs on inhibition of fouling

Fig. 3 shows the effect of MBs supply condition on the water flux of BSA aqueous solution. In Case 2, the MBs were supplied to the membrane, but the over flow and the retentate were not returned to the feed tank. On the other hand, in Case 1, the MBs were not supplied to the membrane, but the over flow and the retentate were returned to the feed tank. It is found from Fig. 3 that the water flux in Case 2 was similar to that in the blank test, Case 1. The reason for this phenomenon is probably that the adsorption speed of BSA onto the MBs is slow and the retention time of MBs in the module is very short, about 1.7 s. Thus, the effect of

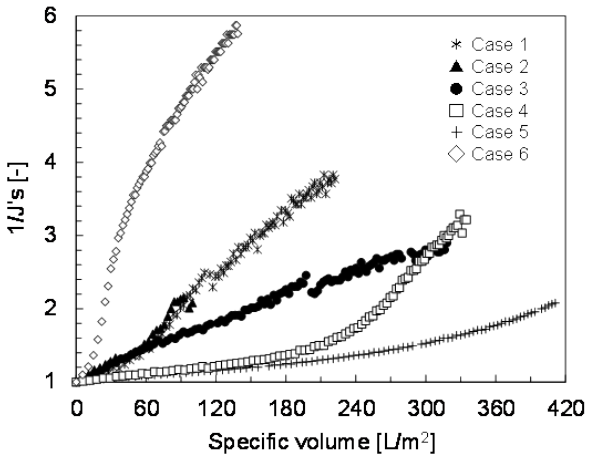

Fig. 3. Effect of microbubble supply condition on the water flux of BSA aqueous solution. The experimental conditions in Case 1–6 are shown in Table 1.

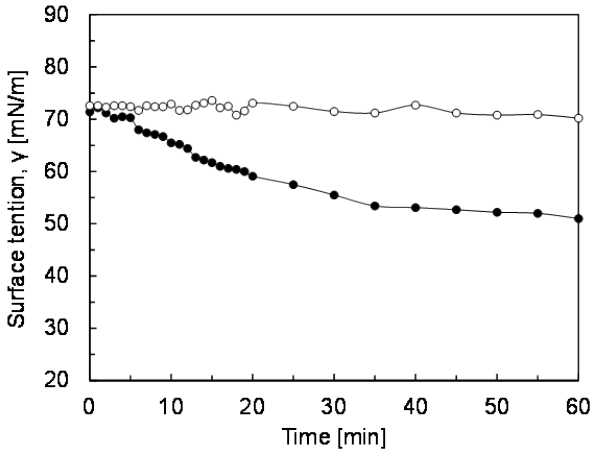

Fig. 4. Time course of the surface tension of BSA solution (closed circles) and pure water (open circles).

MBs is not clear in this condition. To confirm this concept, the adsorption of BSA on the air/liquid interface and on the membrane surface were measured. Figs. 4 and 5 show the time course of the surface tension of BSA solution and the adsorbed amount of model foulants including BSA on CA sensor, respectively. As shown in Fig. 4, the surface tension of pure water was constant, which showed that evaporation of water did not affect the surface tension. On the other hand, the surface tension of the BSA solution decreased slowly for about 35 min and became almost constant, indicating the adsorption speed of BSA onto air/liquid interface was very slow. In addition, it was clear from Fig. 5 that the adsorption amount of BSA onto CA membrane surface was very low compared with Guar-Gum and SR-HA.

In Case 3 in which the over flow and the retentate were returned to the feed tank, the fouling was decreased compared with those in Cases 1 and 2, since the gradient of Case 3 in Fig. 3 was smaller than those of Cases 1 and 2. This result indicate that the fouling is decreased by return-

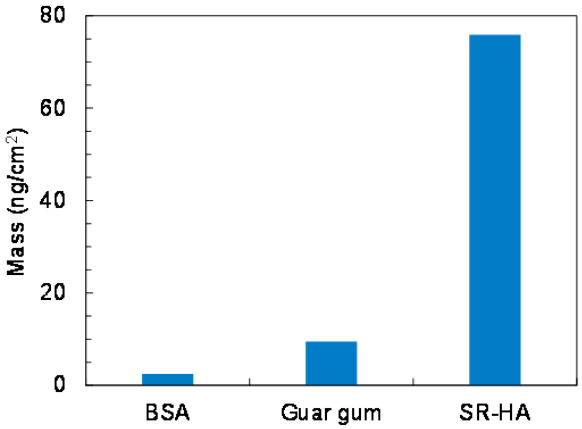

Fig. 5. Adsorbed amount of model foulants including BSA on cellulose acetate membrane surface.

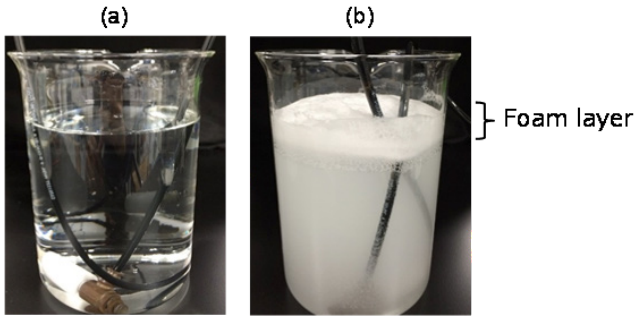

Fig. 6. Feed tank (a) before filtration and (b) after 30 min filtration in Case 3.

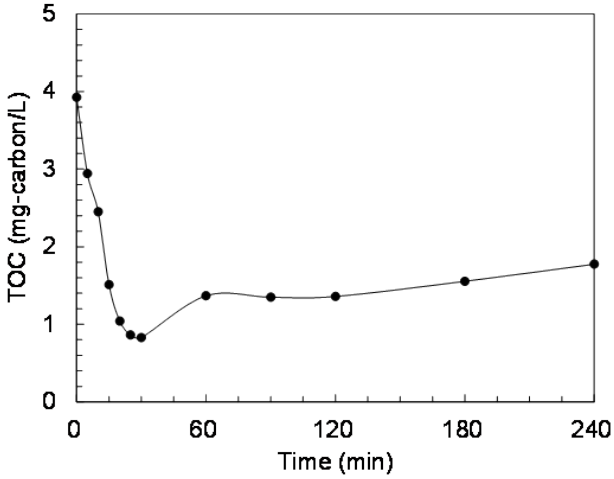

Fig. 7. Time course of total organic carbon at the bottom of feed tank in Case 3.

ing the over flow and the retentate to the feed tank. Figs. 6 and 7 show the feed tank and the time course of TOC at the bottom of feed tank in Case 3, respectively. It is found from Fig. 6 that the foam layer is formed at the upper part of feed tank by the flotation of MBs returned into the feed tank. In addition, the BSA concentration decreased at the bottom of feed tank along with the formation of foam layer. This indicates that the fouling will be decreased by decreasing the foulant concentration using MBs for pretreatment.

In order to confirm this concept, the MBs were used for pretreatment (Case 4). For the pretreatment, MBs was supplied for 30 min, but all solution was directly returned into the feed tank. In Case 4, BSA concentration was 2 ppm at the bottom of feed tank. In parallel, the feed solution of low BSA concentration comparable with Case 4 (TOC: 0.8 mg-carbon/L (=2 ppm protein)) was used as in Case 5 in which no MBs was supplied. The time course of water flux in Case 4 was almost the same as that in Case 5 until 120 L/m^2 of the specific volume. However, the fouling was more accelerated over 300 L/m^2 comparing with Case 3, since the gradient of Case 4 in Fig. 3 was larger than that of Case 3 over 200 L/m^2 and $1/J'_s$ was larger than that of Case 3 over 300 l/m^2. In addition, the foam layer was formed in Case 4 (Fig. 6), but not in Case 5. These facts indicate that the foam layer formed at the upper part of feed tank affects the fouling.

The foam layer is the aggregation of insolubilized BSA. It is found from Fig. 7 that the TOC slightly increases after 60 min, indicating BSA aggregation dissolves into the feed solution. Thus, it is important to make clear the correlation between the formation of BSA aggregation and the fouling. This is discussed in the next section.

3.2. Correlation between the fouling and the coagulation of BSA due to MBs

As discussed in the previous section, it is speculated from Fig. 7 that BSA aggregation dissolves again into the feed solution. In order to confirm this concept, the BSA aggregates were forced to be dispersed due to convection by replacing the suction nozzle to the upper part of feed tank in Case 6. As a result, Case 6 showed the most severe fouling compared with other experimental conditions as shown in Fig. 3.

Fig. 8 shows the TOC at the bottom of feed tank in Cases 1, 4 and 6. It was found from Fig. 8 that, in Case 6, the foam layer almost dissolved (or dispersed) into the feed solution and the TOC in Case 6 was comparable with that in Case 1. Fig. 9 shows the aggregate size distribution of BSA aqueous solutions used in Cases 1, 4 and 6. It was found from Fig. 9 that the number of aggregations with 100–200 nm diameter was remarkably increased. Thus, it is reasonable to consider that, in Case 6, the fouling is increased by the precipitation of BSA aggregations dispersed from foam layer onto the membrane surface.

In addition, it was found from CD spectra shown in Fig. 10 that BSA was denatured by the pretreatment with MBs. It is known that BSA changes the conformation of high-order structure when it adsorbs onto a hydrophobic solid surface [26]. In addition, it is reported that substances adsorbed onto the air/liquid interface precipitate by local condensation when MBs shrink [27]. It is not clear if the denaturation of BSA takes place by local condensation. However, at least, it is obvious that BSA is denatured by the pretreatment with MBs.

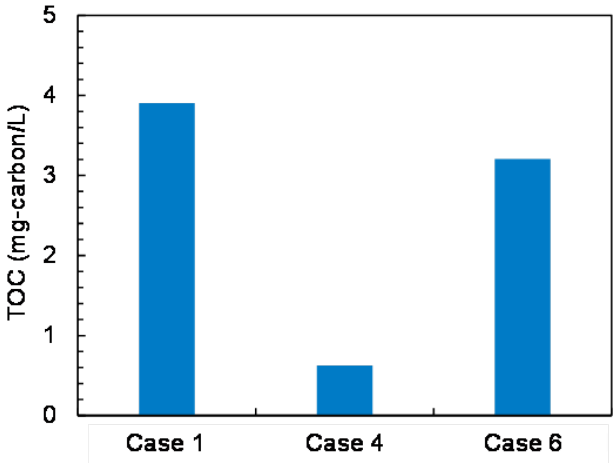

Fig. 8. Total organic carbon at the bottom of feed tank in Cases 1, 4 and 6.

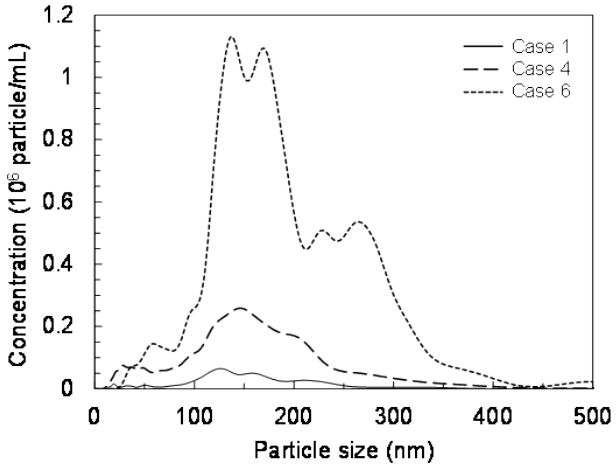

Fig. 9. Particle size distribution of BSA aqueous solutions used in Cases 1, 4 and 6.

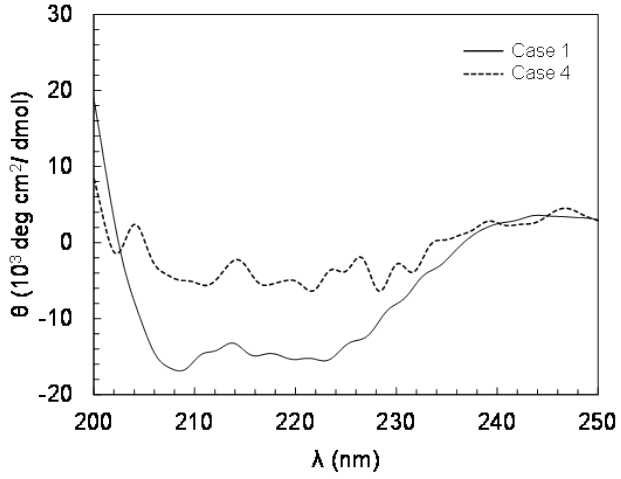

Fig. 10. CD spectra of BSA aqueous solution in Cases 1 and 4.

4. Conclusion

In this study, the mechanism of reducing fouling, especially the fouling due to proteins, by MBs was investigated using bovine serum albumin (BSA) as a model foulant. It was found that MBs had no effect on the fouling reduction, in the case where the retentate and the overflow were not returned into the feed tank. On the other hand, in the case where the retentate and the overflow were returned into the feed tank, BSA was denatured and coagulated by MBs, and then, the coagulated BSA floated in the feed tank. It resulted in the decrease of effective BSA concentration at the bottom of feed tank. Thus, in the case where the feed was suctioned from the bottom of feed tank, the fouling was reduced. However, in the case where the feed was suctioned from the top part of feed tank, the coagulated BSA was also supplied into UF module resulting in the facilitated fouling.

That is, the reduction of fouling by MBs was caused by a decrease in the effective foulant concentration by MBs.

Acknowledgement

This work was partly supported by Grants-in-Aid from the Special Coordination Fund for Promoting Science and Technology, Creation of Innovation Centers for Advanced Interdisciplinary Research Areas (Innovative Bioproduction, Kobe), and the Regional Innovation Strategy Support Program from the MEXT, Japan.

References

[1] N. Lee, G. Amy, J.P. Croue, H. Buisson, Identification and understanding of fouling in low-pressure membrane (MF/UF) filtration by natural organic matter (NOM), Water Res., 38 (2004) 4511–4523.
[2] N. Lee, G. Amy, J.P. Croue, H. Buisson, Morphological analyses of natural organic matter (NOM) fouling of low-pressure membranes (MF/UF), J. Membr. Sci., 261 (2005) 7–16.
[3] C. Jucker, M.M. Clark, Adsorption of aquatic humic substances on hydrophobic ultrafiltration membranes, J. Membr. Sci., 97 (1994) 37–52.
[4] S. Hasegawa, T. Iwamoto, T. Miyoshi, S. Onoda, K. Morita, R. Takagi, H. Matsuyama, Effect of biological contact filters (BCFs) on membrane fouling in drinking water treatment system, Water, 9(12) (2017) 981, 1–10.
[5] I. Kiyosawa, Progress in recent researches on the whey protein concentrates and their functional properties, Milk Science, 51 (2002) 13–26.
[6] H. Chang, H. Liang, F. Qu, B. Liu, H. Yu, X. Du, G. Li, S.A. Snyder, Hydraulic backwashing for low-pressure membranes in drinking water treatment: A review, J. Membr. Sci., 540 (2017) 362–380.
[7] A.H. Nguyen, J.E. Tobiason, K.J. Howe, Fouling indices for low pressure hollow fiber membrane performance assessment, Water Res., 45 (2011) 2627–2637.
[8] W. Gao, H. Liang, J. Ma, M. Han, Z.-L. Chen, Z.-S. Han, G.-B. Li, Membrane fouling control in ultrafiltration technology for drinking water production: A review, Desalination, 272 (2011) 1–8.
[9] H. Huang, K. Schwab, J.G. Jacangelo, Pretreatment for low pressure membranes in water treatment: a review, Environ. Sci. Technol., 43 (2009) 3011–3019.
[10] S.J. Judd, P. Hillis, Optimization of combined coagulation and microfiltration for water treatment, Water Res., 35 (2001) 2895–2904.

[11] Y. Soffer, J. Gilron, A. Adin, Streaming potential and SEM-EDX study of UF membranes fouled by colloidal iron, Desalination, 146 (2002) 115–121.
[12] C. Hallé, P.M. Huck, S. Peldszus, J. Haberkamp, M. Jekel, Assessing the performance of biological filtration as pretreatment to low pressure membranes for drinking water, Environ. Sci. Technol., 43 (2009) 3878–3884.
[13] S. Muthukumaran, K. Yang, A. Seuren, S. Kentish, M. Ashokkumar, G.W. Stevens, F. Grieser, The use of ultrasonic cleaning for ultrafiltration membranes in the dairy industry, Sep. Purif. Technol., 39 (2004) 99–107.
[14] T. Watabe, T. Takahashi, K. Matsuyama, H. Matsuyama, Effect of the addition of fine bubbles on reversible and irreversible membrane fouling in surface water treatment, Desal. Water Treat., 78 (2017) 12–18.
[15] T. Watabe, K. Matsuyama, T. Takahashi, H. Matsuyama, Use of microbubbles to reduce membrane fouling during water filtration, Desal. Water Treat., 57 (2016) 3820–3826.
[16] B. Ma, X. Wang, C. Hu, W.A. Jefferson, H. Liu, J. Qu, Antifouling by pre-deposited Al hydrolytic flocs on ultrafiltration membrane in the presence of humic acid and bovine serum albumin, J. Membr. Sci., 538 (2017) 34–40.
[17] H. Carrere, A. Schaffer, F. Rene, Cross-flow filtration of guar gum solutions: Experimental results, Sep. Purif. Technol., 14 (1998) 59–67.
[18] A.H. Nguyen, J.E. Tobiason, K.J. Howe, Fouling indices for low pressure hollow fiber membrane performance assessment, Water Res., 45 (2011) 2627–2637.
[19] H. Huang, T.A. Young, J.G. Jacangelo, Unified membrane fouling index for low pressure membrane filtration of natural waters: principles and methodology, Environ. Sci. Technol., 42 (2008) 714–720.
[20] K. Kimura, K. Tanaka, Y. Watanabe, Microfiltration of different surface waters with/without coagulation: Clear correlations between membrane fouling and hydrophilic biopolymers, Water Res., 49 (2014) 434–443.
[21] D.T. Myat, M. Mergen, O. Zhao, M.B. Stewart, J.D. Orbell, S. Gray, Characterisation of organic matter in IX and PACl treated wastewater in relation to the fouling of a hydrophobic polypropylene membrane, Water Res., 46 (2012) 5151–5164.
[22] S.Y. Lin, T.L. Lu, W.B. Hwang, Adsorption kinetics of decanolat the air-water interface, Langmuir, 11 (1996) 555–562.
[23] S.N. Moorkanikkara, D. Blankschtein, Possible existence of convective currents in surfactant bulk solution in experimental pendant-bubble dynamic surface tension measurements, Langmuir, 25 (2009) 1434–1444.
[24] N.J. Greenfield, Using circular dichroism spectra to estimate protein secondary structure, Nature Protocols, 1 (2007) 2876–2890.
[25] Z.G. Peng, K. Hidajat, M.S. Uddin, Conformational change of adsorbed and desorbed bovine serum albumin on nano-sized magnetic particles, Colloids Surfaces B: Biointerfaces, 33 (2004) 15–21.
[26] A. Cifuentes, S. Borrós, Comparison of two different plasma surface-modification techniques for the covalent immobilization of protein monolayers, Langmuir, 29 (2013) 6645–6651.
[27] K. Terasaka, Japan Patent Kokai 2009-131737 (18, June, 2009).